| Object | Line | (GHz) | Stokes $V$ (Jy/beam) |
|---|---|---|---|
| **Orion KL** | CO ($J = 3 \rightarrow 2$) | 345.8 | 0.65 |
| | SiO ($J = 8 \rightarrow 7$) | 347.3 | -0.65 |
| **NGC7538** | CO ($J = 3 \rightarrow 2$) | 345.8 | 0.85 |
| **IRC+10216** | CS ($J = 7 \rightarrow 6$) | 342.88 | 0.6 |
| | SiS ($J$ =19→18) | 344.78 | 0.2 |
| | $H^{13}CN$ ($J$ =4→3) | 345.34 | 0.8 |
| | CO ($J = 3 \rightarrow 2$) | 345.8 | 0.4 |
| **NGC1333 (IRAS2a)** | CO ($J = 3 \rightarrow 2$) | 345.8 | None |

**Table 2**. Summary of corrected Stokes $V$ signals found. The beam size is determined by the configuration of the antennas array. An intensity for the peak of the Stokes $V$ signal is only given if the peak is noticeably higher than the noise level. The intensity quoted for CO in NGC7538 is before smoothing is applied.

and therefore a potentially false Stokes $V$ signal. The maps are integrated over a narrow frequency band of approximately 2 MHz so any peaks that exist are not washed out by noise in adjacent channels. In the maps for Orion KL and IRC+10216 shown in Figure 2 there are no negative peaks around the peak of Stokes $V$. However in NGC7538 there is quite a large negative Stokes $V$ peak near our chosen peak that may indicate squint. The top panel of Figure 1 shows ~~what 'squint peaks' look like~~ a typical appearance for squint signals ~~(we know these peaks are from squint because they~~ which disappear after correction), and the pairs tend to resemble each other in shape. The pair of peaks around our chosen peak in NGC7538 however have distinct shapes. The worst case here is that the signal is entirely squint but on the other hand the signal may be a mixture of real and heavily affected by squint. The detections in Orion KL and IRC+10216 are more reliable.

## 5. DISCUSSION

The first question to address is whether our CP detections are real or result from instrumental artifacts. This is our chief concern because of the difficulty ~~of~~ in calibrating CP measurements, especially since the observations presented here were not made with any special considerations for calibrating CP as in the observation of Sgr A* reported in Muñoz et al. (2012). We will repeat here the arguments made in Section 4 in support for the soundness of these detections. We then discuss earlier detections of CP and summarize how ARS can explain the detections presented in this work.

Firstly, we take the average of all the visibility data and note that the peak Stokes $V$ is not proportional to the peak Stokes $I$ at any particular frequency. For example, a large Stokes $I$ at 347.25GHz does not indicate a corresponding peak in Stokes $V$. This property indicates that there is no ~~significant~~ systematic leakage of Stokes $I$ into Stokes $V$. This is true in Orion KL, where CO ($J = 3 \rightarrow 2$) and SiO ($J = 8 \rightarrow 7$) are the strongest lines, and the SiO ($J = 8 \rightarrow 7$) line is stronger. Therefore, if the Stokes $V$ signal were purely leakage from Stokes $I$ then we would expect to see an SiO Stokes $V$ signal that is stronger than the CO Stokes $V$ signal in the visibilities, but we do not; the Stokes $V$ signal from CO ($J = 3 \rightarrow 2$) is stronger. This is also true in the visibilities of IRC+10216, where the CS ($J = 7 \rightarrow 6$) and SiS ($J = 19 \rightarrow 18$) lines have similar strengths but the Stokes $V$ at SiS ($J = 19 \rightarrow 18$) is twice as intense. However, in the same object $H^{13}CN$ ($J = 4 \rightarrow 3$) and CO ($J = 3 \rightarrow 2$) have Stokes $V$ intensities that appear proportional to their Stokes $I$ intensity (stronger $I$ means stronger $V$).

We also note that for Orion KL the shapes of the Stokes $V$ signals vary across the frequency band and interpret this to mean that the signals are not instrumental in nature, assuming that any instrumental mechanism for producing spurious Stokes $V$ produces a single type of CP (left or right). For example Figure 5 shows a spectrum for that source with Stokes $V$ in CO and SiO. The SiO signal is purely negative (indicating only left-circular polarization) but the CO signal is antisymmetric, indicating the presence of both LCP and RCP. This has a physical explanation using the ARS model in terms of blue-shifted and red-shifted scattering populations that will be considered in Section 5.2. We know of no instrumental mechanism for producing such a signature. For the other objects the Stokes $V$ signal is always positive.

In the case of IRC+10216, an evolved carbon star with an extended envelope, we note that the peak of Stokes $V$ in the CO ($J = 3 \rightarrow 2$) map (bottom-right panel of Figure 2) is ~~roughly~~ approximately 6" away from the Stokes $I$ emission, and were concerned that the Stokes $V$ peak was not even on the object. From single-dish CO ($J = 2 \rightarrow 1$) observations of the shell around IRC+10216 we find the radius of the CO shell to be 50" (Fig. 1 of Cernicharo et al. 2015), indicating that the Stokes $V$ signal is indeed on the object.

Spatial filtering due to the resolution of the interferometer explains the ~~much smaller radius~~ smaller spatial extent of IRC+10216 in the observations presented here and also explains the frequent occurences of negative Stokes $I$ in almost all the spectra shown in Figures 2, 3, and 5, as well as the ~~extremely~~ high levels of CP ~~that range~~ varying from 6% to 30%. The largest resolvable ~~object~~ scale by an interferomter is determined by the length of the shortest baseline, meaning that large scale emission can be ~~invisible to~~ filtered out by the interfer-

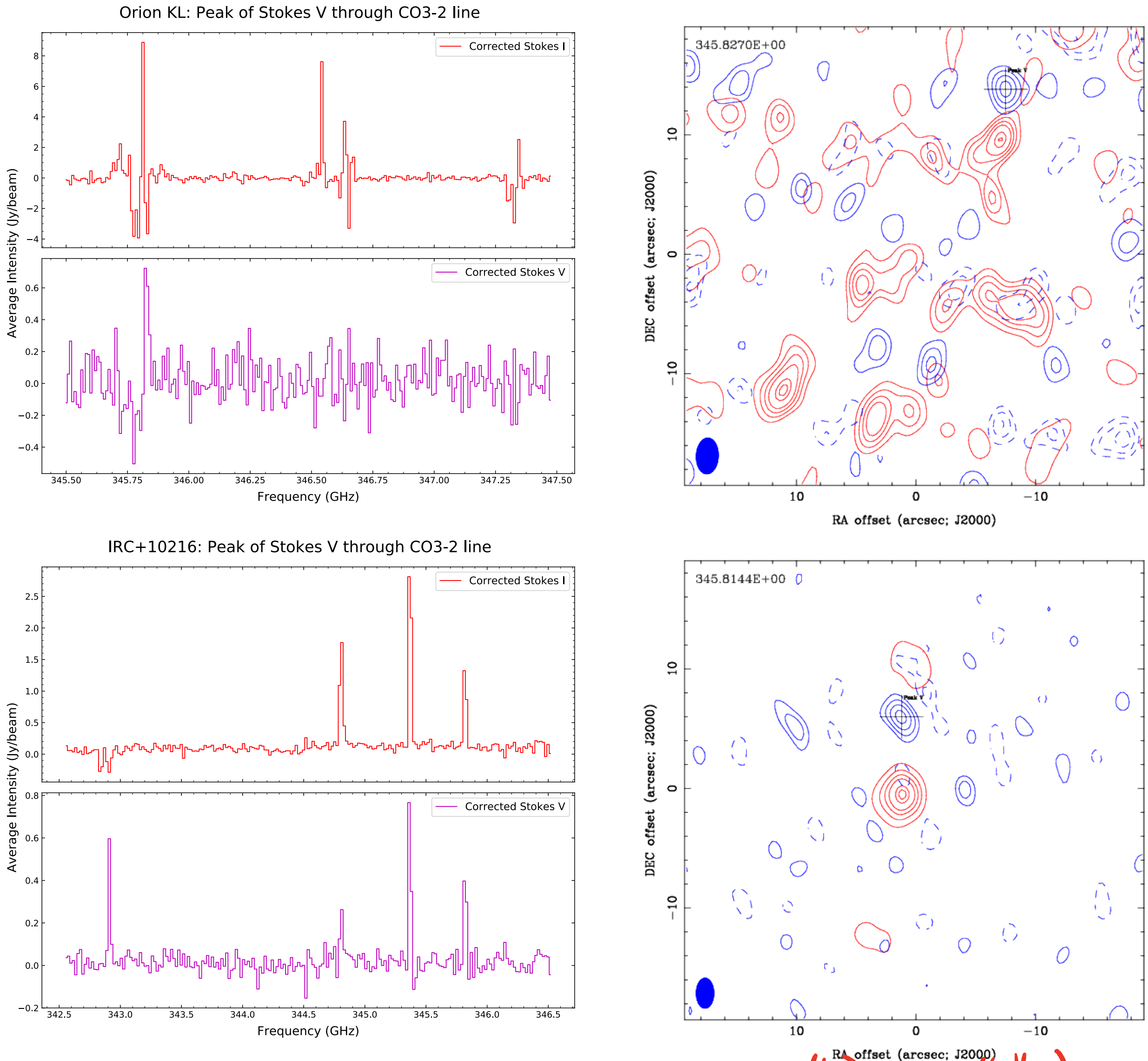


**Figure 2**. Corrected spectra and maps of the CO ($J = 3 \rightarrow 2$) line (345.8GHz) for Orion KL (top) and IRC+10216 (bottom). ***Spectra*:** *Miriad*'s `maxfit` is used on the CO map to obtain the location on the image where the Stokes $V$ signal at 345.8GHz is maximum, and a spectrum is obtained through that point. The cross on the map denotes the location of that peak. The red line is Stokes $I$ and the blue is Stokes $V$. ***Maps*:** Blue contours are Stokes $V$ and are shown at the -4, -3, -2, 2, 3, 4$\sigma$ levels. The RMS error for each Stokes $V$ map is found using *Miriad*'s `imstat` command: $\sigma = 0.30$ and 0.17 Jy/beam, for Orion KL and IRC+10216, respectively. Dark red contours are Stokes $I$ and the levels are 15%, 30%, 45%, 60%, 85% and 95% of the maximum. The value in the top left is the central frequency of the mapped signal in GHz, ~~and the map is~~ integrated over a narrow bandwidth of $\sim$2 MHz.

ometer. For example in Orion KL the CO ($J = 3 \rightarrow 2$) Stokes $I$ emission is large and extended. If ~~then~~ the Stokes $V$ signal came ~~comes~~ from smaller ~~more~~ localized areas, then we would observe peaks of Stokes $V$ as shown while ~~and~~ only a portion of the Stokes $I$ would be ~~that is~~ present. The rest of the Stokes $I$ signal, would be filtered away, which could shift the zero-level downward ~~to smaller values~~. Fluctuations in Stokes $I$ could ~~would~~ then appear to have negative values. The smaller Stokes $I$ could ~~would~~ also explains the high levels of $V/I$ observed.

Finally we checked and confirmed that there were no Stokes $V$ signals in the continuum larger than those found in ~~at~~ molecular lines like CO and SiO. If the detected CP originated ~~originates~~ from instrumental artifacts then we would detect CP at similar levels in the continuum, but this is not seen. The level of CP found in ~~at~~ molecular transitions is always higher than the level of CP in the continuum for the observations presented here.

We therefore feel confident that the CP reported here, although perhaps suffering from some level of instrumental contamination, is real and originate from within ~~each of~~ these objects. However, it still remains ~~It is thus~~ important to improve the measurement and calibration of CP for future studies of magnetic fields using polarimetry.

### 5.1. Non-Zeeman CP *Earlier Detections*

CP ~~Circular polarization~~ in a molecular spectral line weakly sensitive to the Zeeman effect was first reported by ~~in~~ Houde et al. (2013), where approximately ~~roughly~~ 2% polarization ~~CP~~ was de-

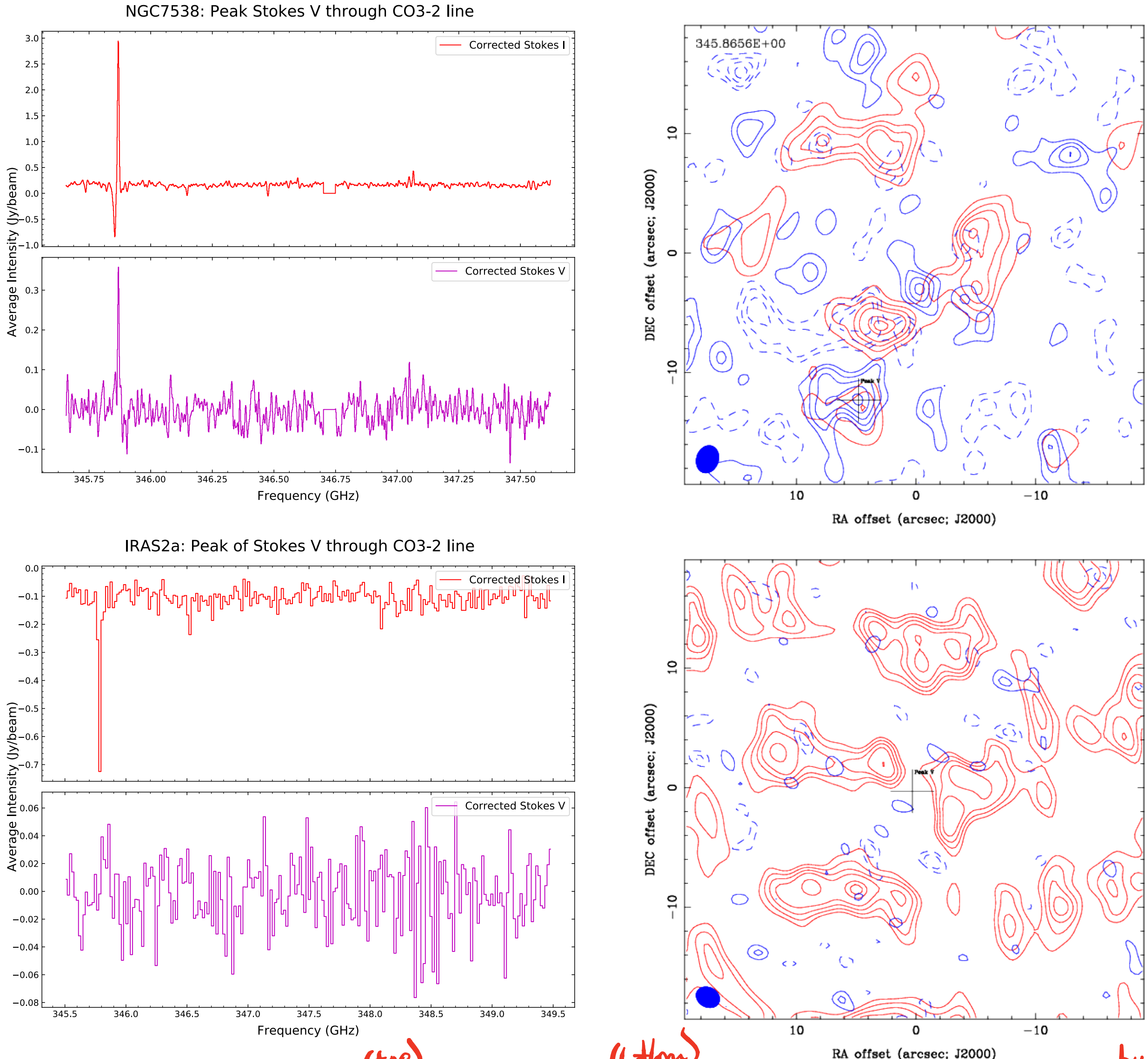


(top) (bottom) by ~

**Figure 3**. Same as Figure 2 but for NGC7538 and NGC1333 (IRAS2A). The spectrum for NGC7538 is Hanning smoothed. No significant Stokes $V$ signal is detected in NGC7538~~, probably because the object is too dim~~. Contours are the same levels as in Figure 2 and the spectrum is obtained the same way. The RMS for the NGC7538 map is $\sigma = 0.15$ Jy/beam.

↳ for IRAS2A?

tected in the $^{12}$CO ($J = 2 \rightarrow 1$) transition at 230.5 GHz in Orion KL using the FSPPol at the CSO. The CP signal was approximately symmetric (i.e. "∩"-shaped). The observation was repeated three months after the first measurement to confirm the result was not spurious, with similar results. Additionally the strong line of HCN ($J = 3 \rightarrow 2$) at 265.9 GHz in Orion KL was measured and no CP higher than the 0.1% level was detected. The detection in CO and the absence of a detection in HCN ~~indicates~~ were evidence that the FSPPol/CSO observations were not significantly suffering from leakage into Stokes $V$ and highlighted the CO molecule as a ~~source of~~ target for non-Zeeman CP. In all the objects presented here we find CP in $^{12}$CO ($J = 3 \rightarrow 2$) at 345.8 GHz (except for in NGC1333 where the CO line is relatively weak). This is consistent with the original 2013 detection.

In follow up work Hezareh et al. (2013) examined the supernova remnant IC 443 using dust polarimetry with PolKa at APEX and polarization maps of $^{12}$CO ($J = 2 \rightarrow 1$) and ($J = 1 \rightarrow 0$) taken with the IRAM 30m telescope. They initially found that ~~initially~~ the ~~linear polarization~~ LP maps of dust and CO differed greatly in their polarization angles. Expecting that there was conversion of linear to circular polarization due to ARS, the CO Stokes $V$ fluxes were then reinserted into the CO LP signals. The resulting CO polarization angle maps then agreed very well with each other, as well as with the dust map (Fig. 9 of Hezareh et al. 2013). This result clearly establishes a conversion from linear to circular polarization.

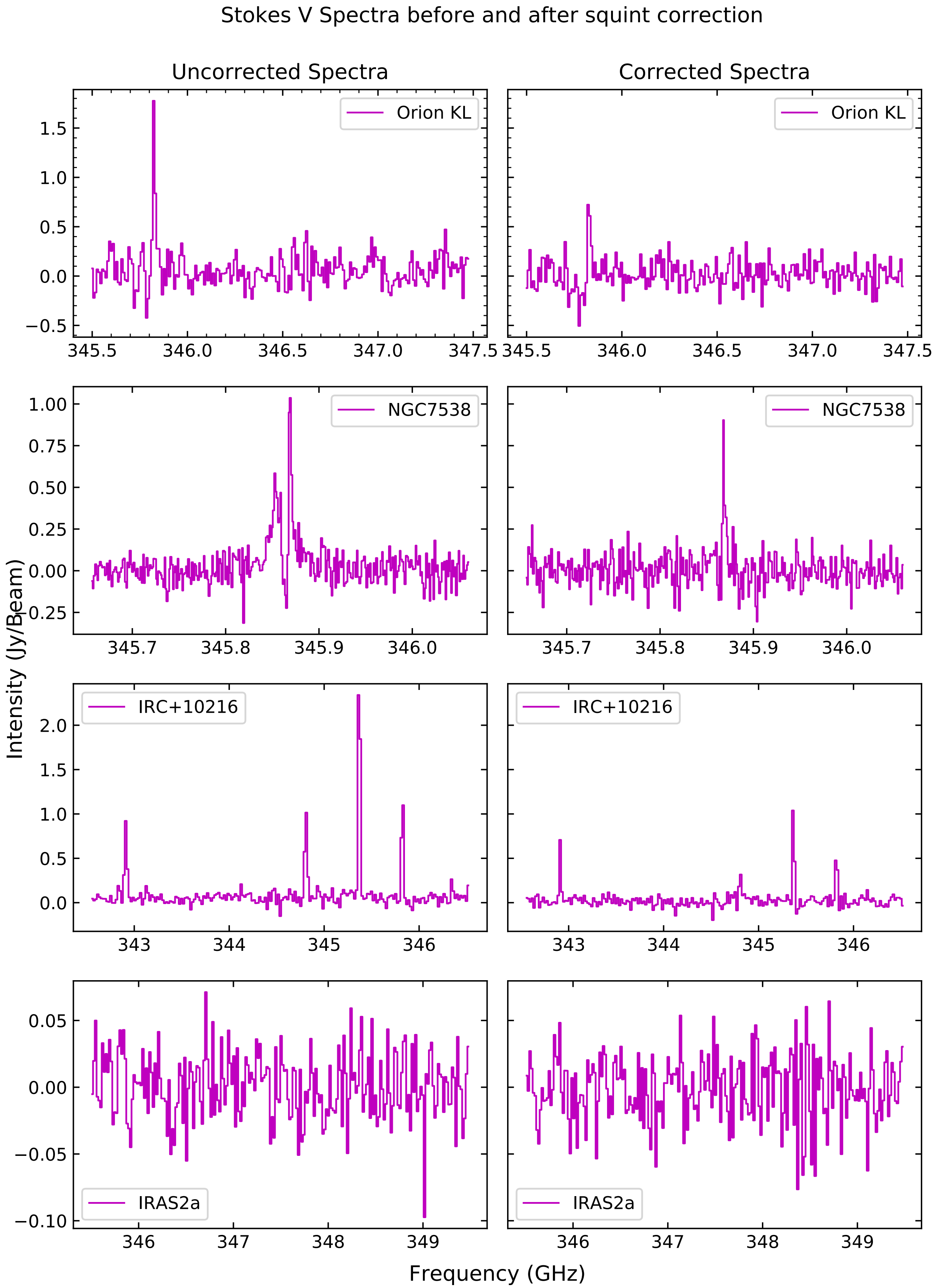


**Figure 4.** Stokes $V$ spectra of all objects before and after squint correction. *Miriad*'s `maxfit` is used on the CO map for each respective object to obtain the location in the image where the Stokes $V$ signal at 345.8GHz is maximum, and a spectrum is obtained through that point. Note that the Stokes $V$ signal decreases in all cases after squint correction.

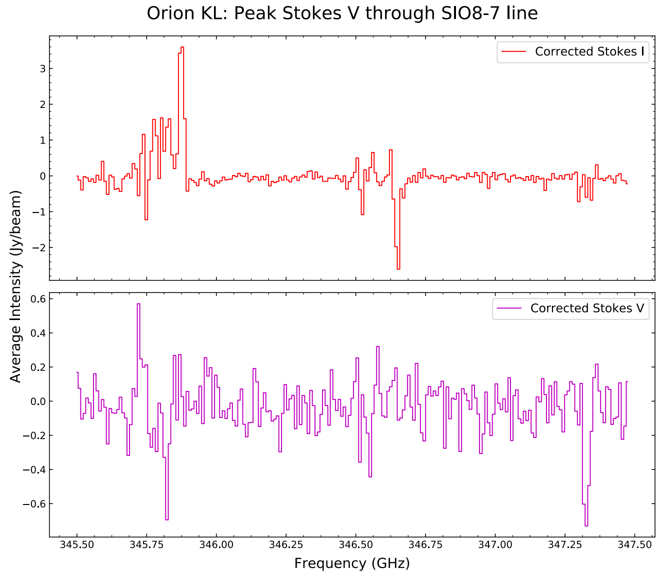


**Figure 5.** Peak Stokes $V$ signal for the SiO ($J = 7 \rightarrow 8$ at 347.3 GHz) transition in Orion KL. Note there is also a strong Stokes $V$ signal in the CO ($J = 3 \rightarrow 2$ at 345.8 GHz) transition here. The SiO signal is purely negative but the CO signal is antisymmetric.

detected are readily explained through ARS off populations of foreground molecules located

### 5.2. *Anisotropic Resonant Scattering*

ARS was the mechanism first proposed by Houde et al. (2013) to explain the presence of CP in the transitions of CO, but initially failed to explain the observed ~~positive and~~ symmetric "∩"-shaped Stokes $V$ profile. In a follow up paper Houde (2014) considered observations of Stokes $V$ in SiO masers and showed that different profile shapes ~~easily arose if there were populations of scattering foreground molecules~~ slightly outside of the velocity range of the line. For example ~~in that case~~, a blue-shifted scattering population of molecules ~~results~~ could result in a negative "∪"-shaped profile ~~and~~ while a red-shifted population ~~results~~ in a positive "∩"-shaped profile. The presence of both a blue- and red-shifted population ~~results in~~ would cause an antisymmetric "S"-shaped profile (like the one seen in the top left panel of Figure 2).

(Cotton, Ragland & Danchi 2011)

The basic principle of ARS can be illustrated by considering ~~linearly polarized~~ background LP radiation oriented at some angle $\theta$ to the foreground magnetic field. The incident and scattered radiation can be written in terms of the $n$-photon states as (Houde et al. 2013)

$$|\psi\rangle = \alpha|n_{||}\rangle + \beta|n_{\perp}\rangle \quad (5)$$

$$|\psi'\rangle \simeq \alpha e^{i\phi}|n_{||}\rangle + \beta|n_{\perp}\rangle, \quad (6)$$

where $\alpha = \cos(\theta)$, $\beta = \sin(\theta)$ and $\phi$ is a phase shift incurred after multiple scattering events. Following the definitions of the Stokes parameters and using an appropriate basis the Stokes parameters for the scattered radiation can be found to be

$$I = \alpha^2 + \beta^2 \quad (7)$$

$$Q = \alpha^2 - \beta^2 \quad (8)$$

$$U = 2\alpha\beta\cos(\phi) \quad (9)$$

$$V = 2\alpha\beta\sin(\phi). \quad (10)$$

This implies that in the chosen basis Stokes $U$ is lost to Stokes $V$. A calculation of the phase shift $\phi$ incurred due to ARS can be found in Houde et al. (2013).

Now, given a conversion from $U$ to $V$ it is clear that measuring $V$ is necessary for techniques like the DCF method that rely on the dispersion of the PAs of LP to calculate the strength of the magnetic field. This is because without corresponding $V$ measurements, the PAs obtained from a molecular spectral line subject to ARS (like CO ($J = 3 \rightarrow 2$)) will be rotated in a ~~complicated~~ systematic way that changes the dispersion of the PAs, as seen in Hezareh et al. (2013). As mentioned earlier, ~~In that study the measured $V$ was re-inserted into $U$ according to~~ LP to CP conversion

~~$U' = U\cos\phi + V\sin\phi$, (11)~~

was reversed ~~where $\phi = \tan^{-1}(V/U)$,~~ to obtain corrected polarization angles. ~~This was shown to work by comparing CO ($J = 2 \rightarrow 1$) polarization maps to dust continuum maps (which is not subject to ARS) and seeing that the two maps only agreed after correction.~~

Because the DCF method relies on the observed dispersion of PAs using LP, ~~from CO maps therefore yields the incorrect value for the magnetic field unless the PAs are corrected~~ (Hezareh et al. 2013; Chandrasekhar & Fermi 1953; Hildebrand et al. 2009). Add Houde et al. (2009)

## 6. CONCLUSION

We analyzed polarimetric observations from the SMA archive of Orion KL, IRC+10216, NGC7538 and NGC1333 ~~and examined them~~ to search for CP signals. The data were corrected for squint, a source of ~~false~~ spurious Stokes $V$ signals that arises due to a slight misalignment in the beams used to obtain Stokes $V$ when performing observations. We found evidence of significant Stokes $V$ in Orion KL, IRC+10216 and NGC7538 in the transitions of CO ($J = 3 \rightarrow 2$), SiO ($J = 8 \rightarrow 7$), CS ($J = 7 \rightarrow 6$), SiS ($J = 19 \rightarrow 18$) and $H^{13}CN$ ($J = 4 \rightarrow 3$). see abstract We measured relatively important levels of CP ranging from 6% to 30% probably due to the interferometric ~~We also obtained much higher percentages of polarization than expected (ranging from 6-30% for $V/I$) due to the~~ spatial filtering of large scale emission.

Theories that explain the presence of non-Zeeman CP in molecular spectral lines rely on the conversion of background LP. The detections in multiple lines and objects presented here indicate that such an effect is likely widespread ~~and common~~ since. The conversion of ~~CP-to-LP~~ LP-to-CP modifies the observed dispersion of PAs, ~~which alters the calculated magnetic field obtained from analyses like the~~ any such studies using molecular lines must also include corresponding CP measurements to account for the polarization conversion effect & determine the needed PAs orientation (citations)



DCF method.

it is necessary to obtain ~~Taking~~ precise measurements ~~observations~~ of CP along with LP for ~~and correcting for this conversion effect is therefore a critical step in~~ corresponding ~~polarization~~ studies of the magnetic field in the interstellar medium.

## REFERENCES


Cernicharo, J., Marcelino, N., Agúndez M., & Guéllin, M. 2015 A&A, 575, A91

Chandrasekhar, S., & Fermi, E. 1953 ApJ, 118, 113

Crutcher, R. M. 2012 Annu. Rev. Astron. Astrophys, 50, 29-63

Goldreich, P., Kylafis, N. D. 1981 ApJ, 243, L75-L78

Hamaker, J. P., Bregman, J. D., & Sault, R. J. 1996 A&A Suppl. Ser., 117, 137-147

Hezareh, T. J., Wiesemeyer, H., Houde, M., Gusdorf, A., Siringo, G. 2013 A&A, 558, A45

Hildebrand, R. G., Kirby, L., Dotson. J. L., Houde, M., Vaillancourt, J. E. 2009 ApJ, 696, 567-573

Houde, M., Hezareh, T., Jones, S., & Rajabi, F. 2013 ApJ, 764, 24

Houde, M. 2014 ApJ, 795, 27

Muñoz, D. J., Marrone, D. P., Moran, J. M., & Rao, R. 2012 ApJ, 745, 115

Marrone D. P. & Rao R. 2008, Proc. SPIE 7020, 70202B

Sault, R. J., Teuben, P. J. & Wright M. C. H. 1995 ADASS IV, ASP Conference Series, 77, 433-436

Sault, R. J., Hamaker, J. P., & Bregman, J., D. 1996 A&A Suppl. Ser., 117, 149-159

Sault, R. J., Killeen, N. 2008, Miriad Users Guide, Australia Telescope National Facility

Schwab, F. R. 1980, Proc. SPIE 0231, Intl Optical Computing Conf I

Thompson, A. R., Moran, J. M., & Swenson Jr, G. W. 2001, Interferometry and synthesis in radio astronomy (John Wiley & Sons)

Vallée, J. P. 2011, New Astronomy Reviews 55, 23–90


we measured relatively important levels of CP ranging from 6% - 30%, probably due to Interferometric spatial ...


Davis, L., Jr. 1951, PhRv, 81, 890

Hezareh, T. & Houde, M. 2010, PASP, 122, 786

Cotton, W.D., Ragland, S., & Danchi, W.C. 2011, ApJ, 736, 96

Houde, M., Vaillancourt, J.E., Hildebrand, R.H., Chitsazzadeh, S., & Kirby, L., 2009, ApJ, 706, 1504